

## **SUPPLEMENTARY INFORMATION**

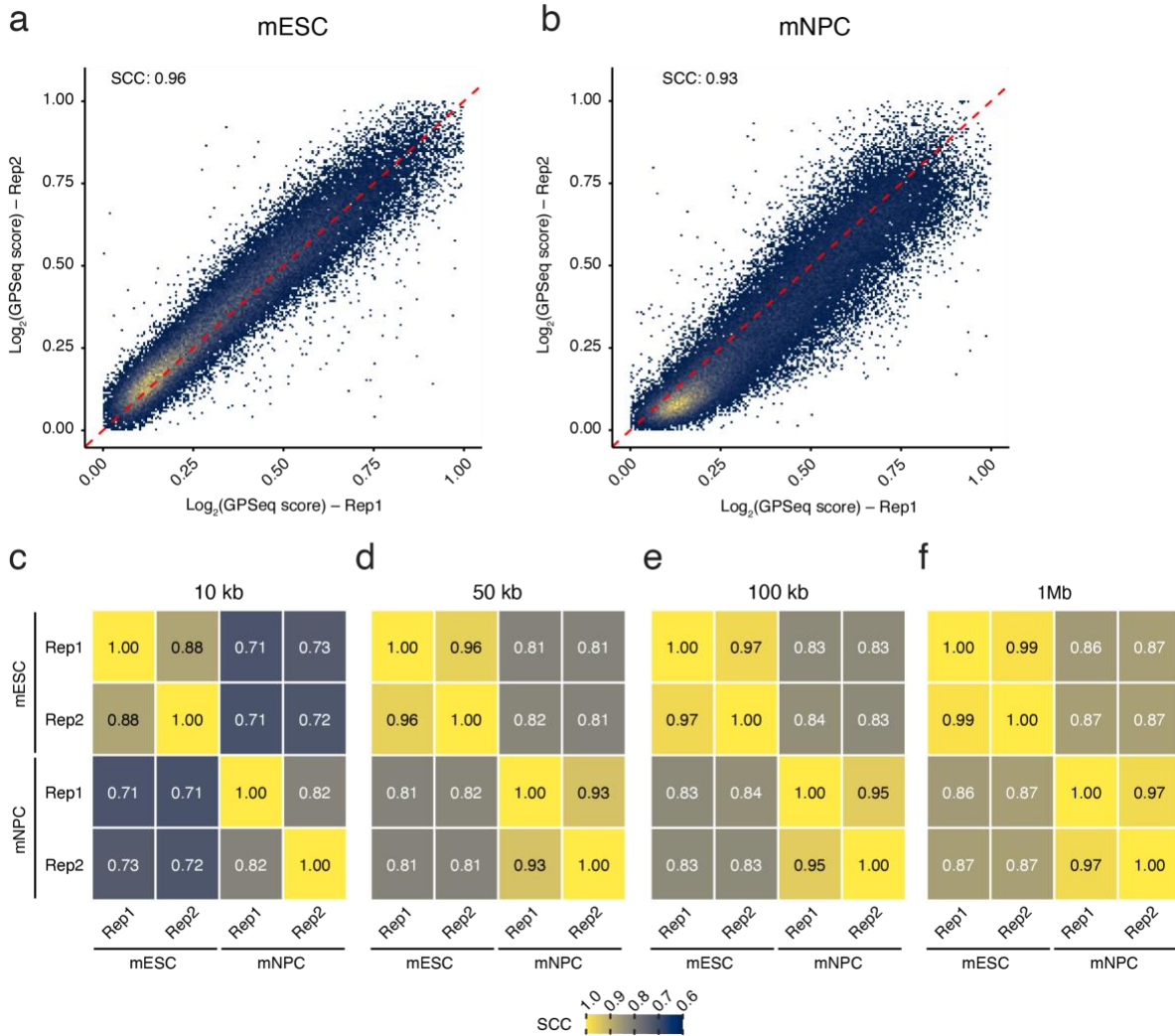
# **Genome-wide and allele-resolved maps of the radial architecture of the mouse genome**

**Lorenzo Salviati, Wing Hin Yip, Giulia Peveri, Agnese Loda, Erik Wernersson,  
Nicola Crosetto, Edith Heard, Britta A. M. Bouwman, Magda Bienko**

- |                          |        |
|--------------------------|--------|
| 1. Supplementary Figures | pg. 2  |
| 2. Supplementary Tables  | pg. 15 |

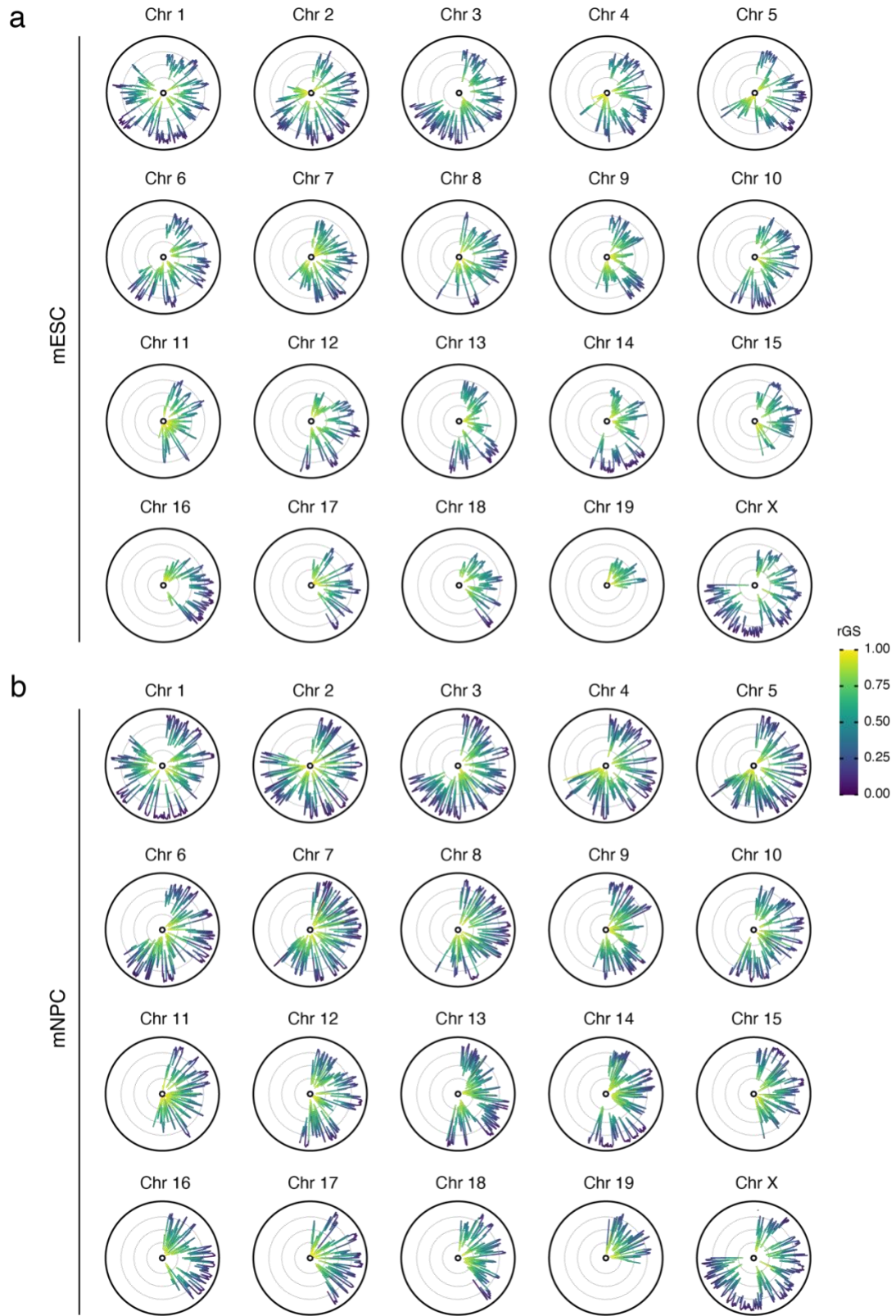
# 1. Supplementary Figures

## Supplementary Figure 1



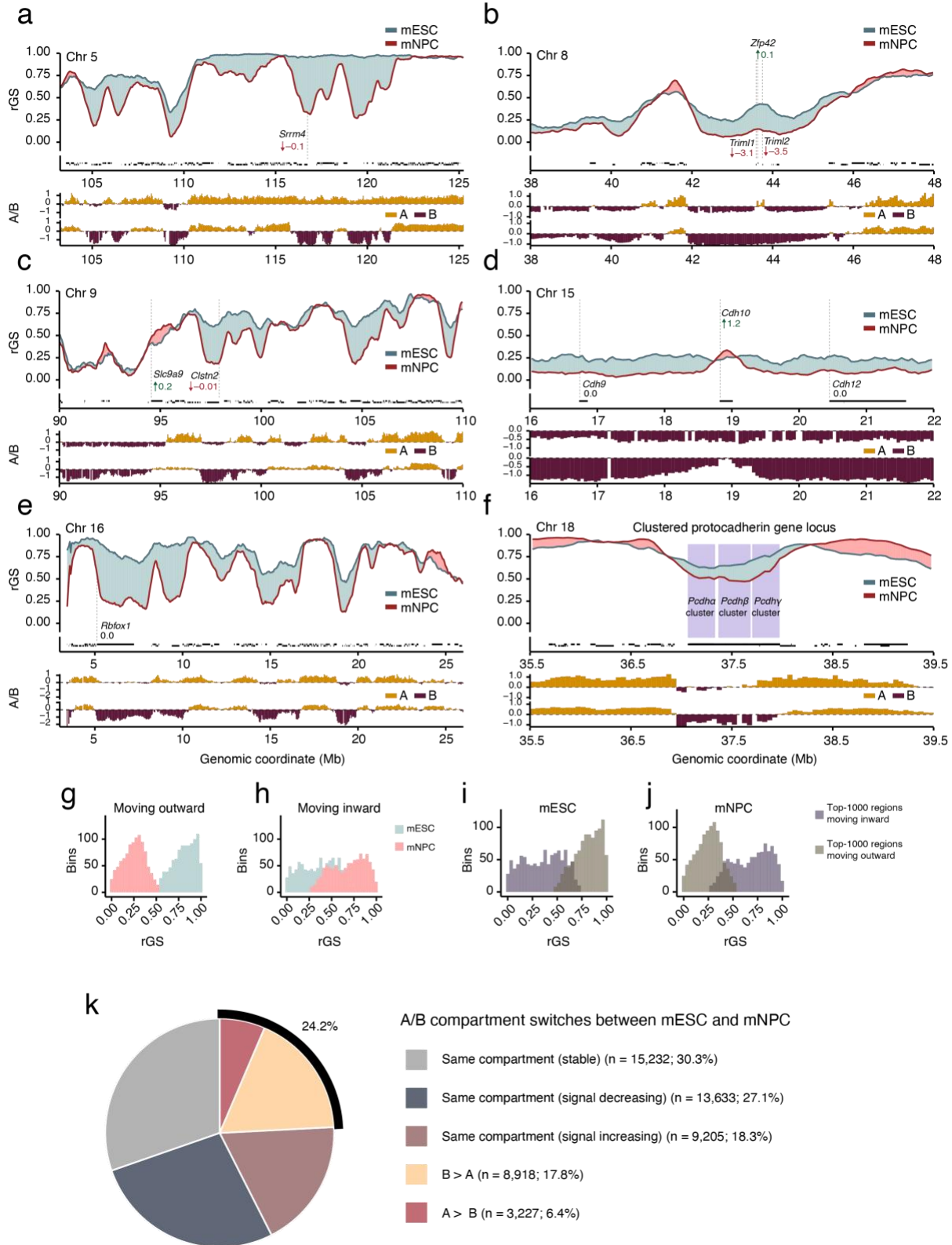
**Supplementary Figure 1. Correlation between GPSeq scores from mESC and mNPC replicates at various resolutions.** (a, b) Correlation between the GPSeq scores of the two GPSeq replicates for each sample, featuring log<sub>2</sub>-scaled GPSeq scores (at 50 kb) in mESC (a) and in mNPC (b). SCC, Spearman's Correlation Coefficient. (c-f) Multi-resolution heatmaps (10kb, 50kb, 100kb, 1Mb) showing Spearman's Correlation Coefficient (SCC) values across all samples and replicates. A link to the Source Data and code to regenerate the plots in this figure is provided in the Data Availability and Code Availability statements.

# Supplementary Figure 2



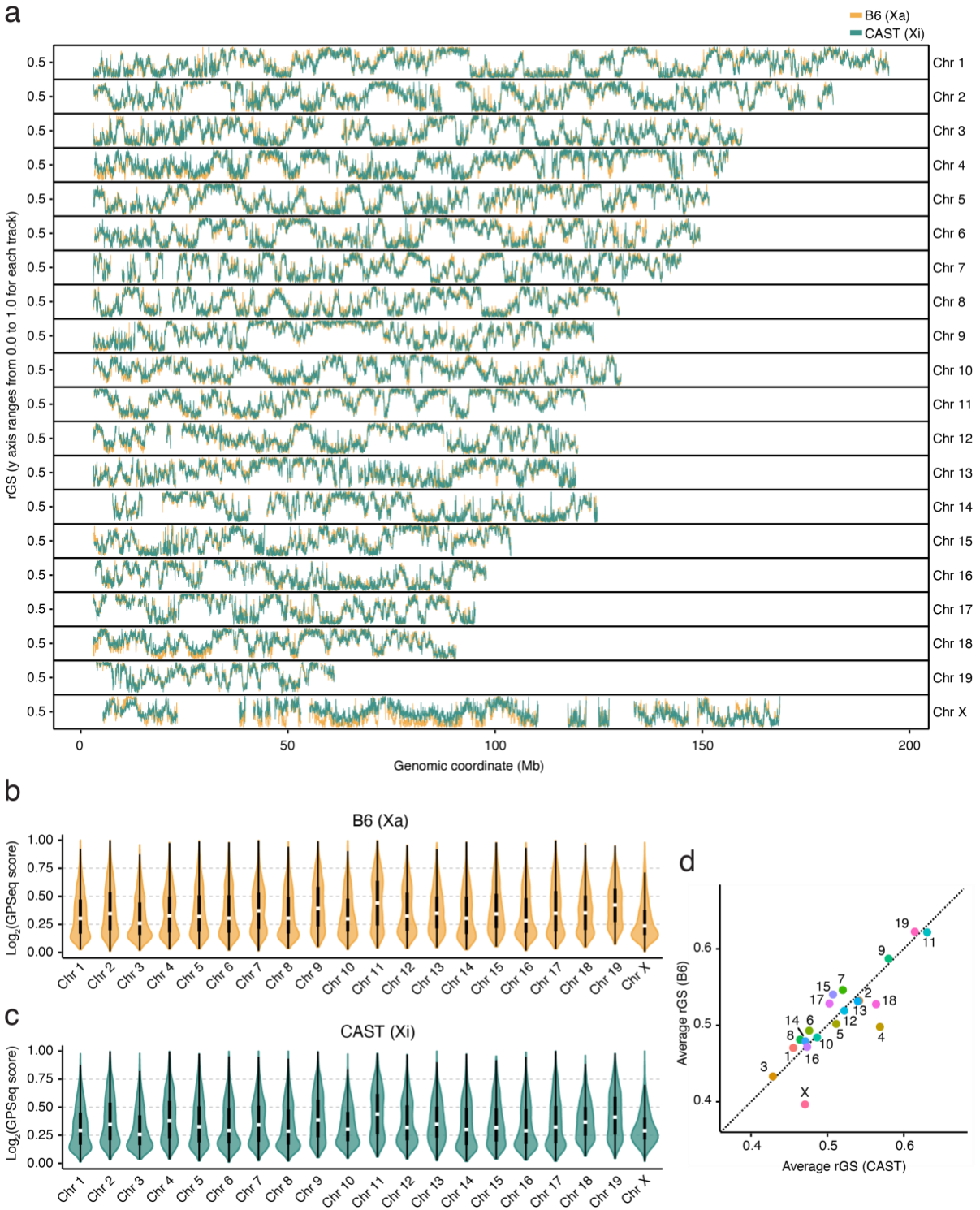
**Supplementary Figure 2. Chromosome-specific high-resolution radially maps in mESC and mNPC. (a, b)** Circular representations of ranked GPSeq score (rGS) values in mESC (a) and mNPC (b). Each chromosome is represented individually, and tracks are colored based on rGS values. Circular grey lines mark 0.25, 0.50 and 0.75 percentiles, respectively, while outer black lines indicate 0 (periphery) and 1 (center). A link to the Source Data and code to regenerate the plots in this figure is provided in the Data Availability and Code Availability statements.

# Supplementary Figure 3



**Supplementary Figure 3. Radial repositioning and A/B compartment switching of genes and regions during neuronal cell lineage specification.** (a-f) Ranked GPSeq score (rGS) profiles (50 kb resolution) across six genomic regions on six different chromosomes, for mESC (blue) and mNPC (red). For visualization, the rGS values were smoothed over 3–6 consecutive genomic bins depending on window size. The area between curves is colored according to the cell type that shows the highest local rGS, indicating positioning closer to the nuclear center. Black horizontal bars, gene bodies. Dashed vertical lines, transcription start site (TSS) of the highlighted genes. Arrows and numbers indicate direction of  $\log_2FC$ , rounded to 1 decimal place. Tracks below rGS profiles show z-scored Hi-C eigenvalues of the corresponding region, indicating active A (yellow) and inactive B compartments (burgundy). (g, h) Distribution of rGS radiality values of the top 1000 regions shown in **Figure 3a, b**, moving inward (g) and outward (h), in mESC (blue bars) and mNPC (red bars). (i, j) Distribution of rGS values of the top 1000 regions shown in **Figure 3a, b**, moving inward (i) and outward (j), in mESC (blue bars) and mNPC (red bars). (k) Pie chart representation summarizing stable and switching regions based on A/B compartment signal variation from mESC to mNPC. Regions switching from A to B are depicted in red, while regions switching from B to A are depicted in yellow. A link to the Source Data and code to regenerate the plots in this figure is provided in the Data Availability and Code Availability statements.

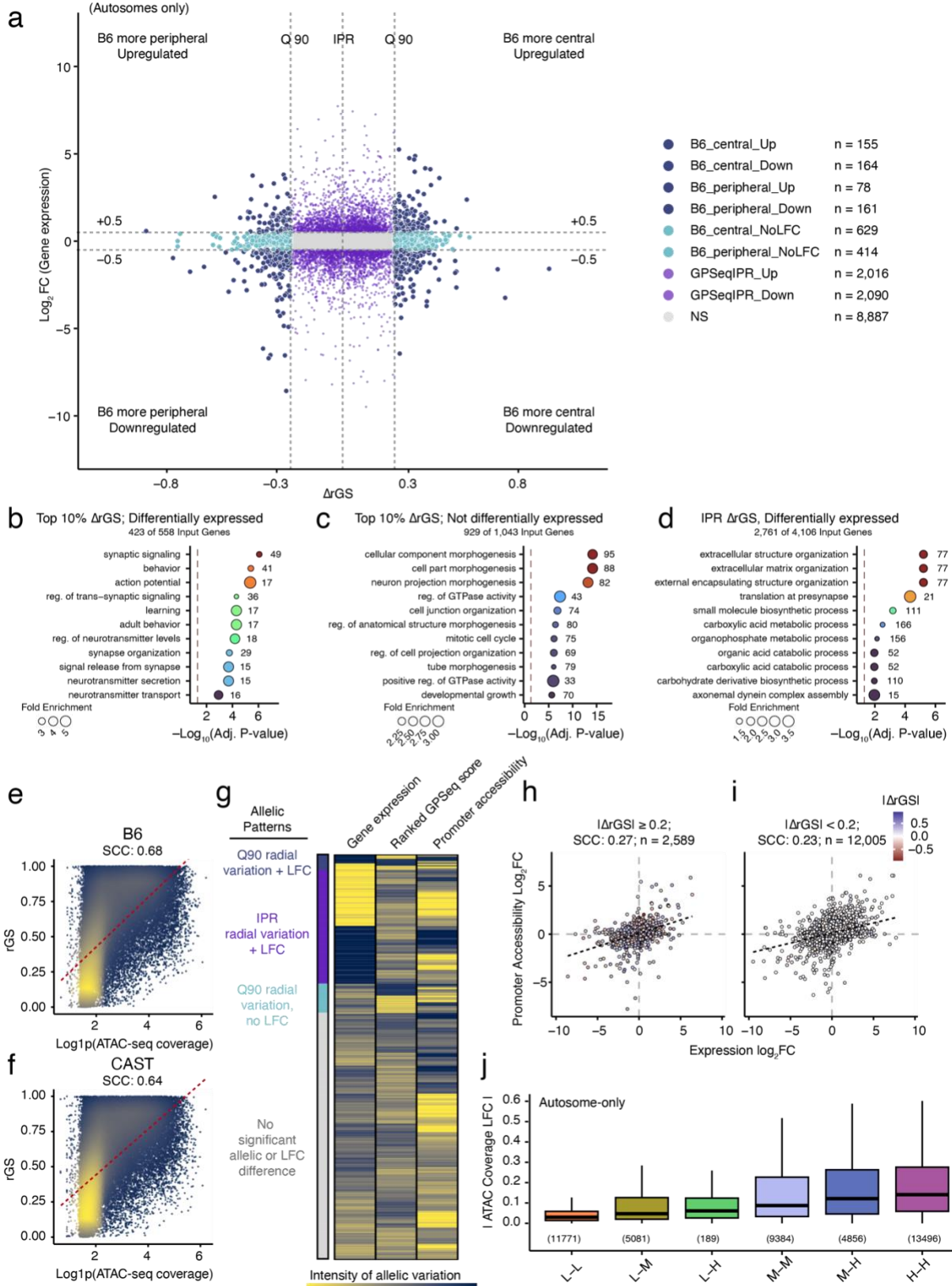
# Supplementary Figure 4



**Supplementary Figure 4. Allelic radiality similarity assessed per chromosome. (a)** Genome-wide representation of ranked GPSeq score (rGS) radiality values of the B6 and CAST alleles at

50kb resolution, per chromosome. Signal mapped to the B6 genome is colored in yellow, while signal mapped to the CAST genome is colored in green. **(b, c)** Violin plots showing distribution and density of the log<sub>2</sub>-scaled GPSeq scores at 50kb resolution for each chromosome, allele-resolved for B6 (b) and CAST (c). In all violin plots, whisker show the range of the data excluding outliers, box spans the 1<sup>st</sup> to 3<sup>rd</sup> quartile, white points indicate the median. **(d)** Average radial positioning of chromosomes in mNPC, allele-resolved. Each dot represents one homologue pair, and radial positioning is expressed as the average of all rGS values along the indicated chromosome ('Chr' is omitted for visibility: e.g., number 3 represents Chr 3) for the B6 allele (y-axis) and the CAST allele (x-axis). A link to the Source Data and code to regenerate the plots in this figure is provided in the Data Availability and Code Availability statements.

# Supplementary Figure 5



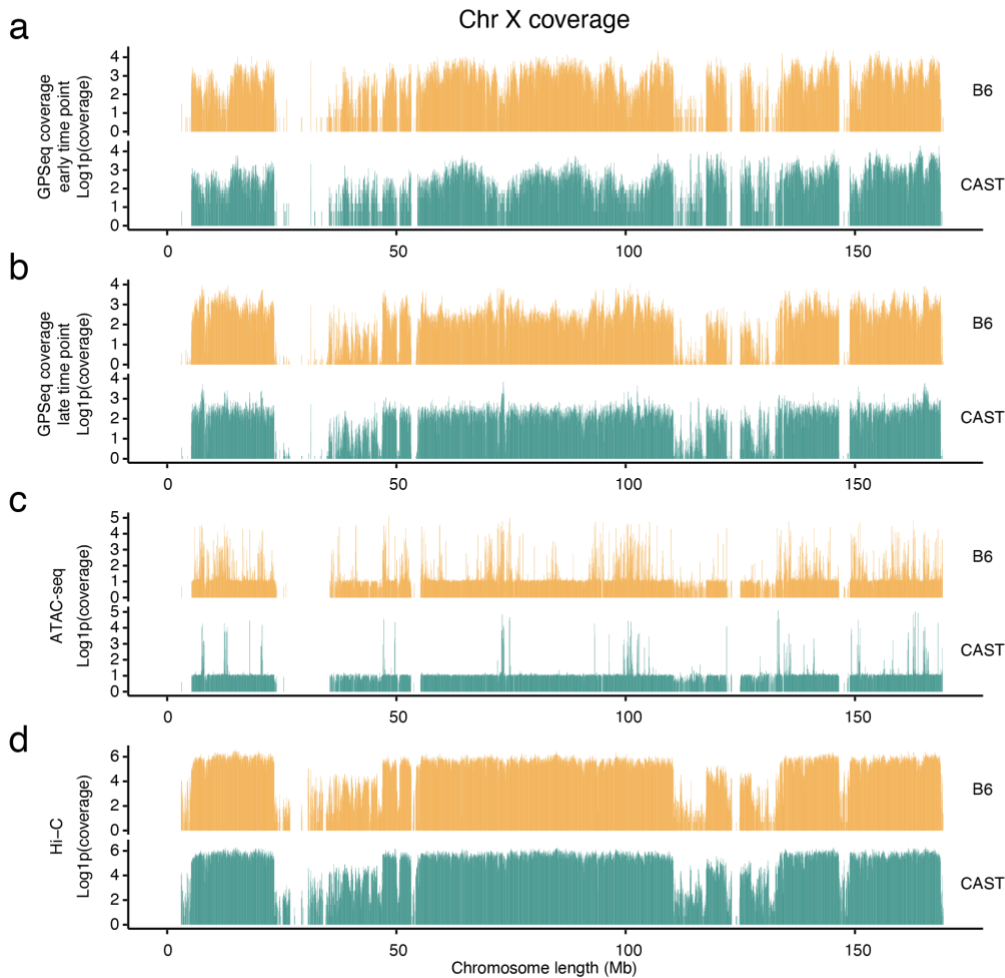
**Supplementary Figure 5. Investigation of allelic radiality variation of autosomes in mNPCs.**

**(a)** Correlation scatterplot of the relationship between differences in radial positioning and gene expression across alleles in autosomes. The y-axis shows gene expression differences as  $\log_2FC$  between B6 and CAST TPM values. The x-axis shows radial positioning changes as the difference between B6 and CAST radiality ( $\Delta rGS$ ). Each dot represents one autosomal gene. Two horizontal dashed lines mark the gene expression thresholds ( $-0.5$  and  $+0.5$ ), while two vertical dashed lines indicate genes with the largest allelic radiality variation (above the 90<sup>th</sup> percentile,  $q90$ ). Genes are colored according to expression and radiality thresholds to identify different groups: i) differential expression and radial placement ( $n = 558$ , dark blue); ii) differential radial placement only ( $n = 1,043$ , light blue); iii) differential expression only ( $n = 4106$ , purple); iv) stable ( $n = 8,887$ , grey).

**(b-d)** Results from Gene Ontology (GO) analysis of autosomal genes found in different groups described in (a): genes with high variation in both expression and radiality ( $n = 558$ ) (b), genes with high variation in radiality only ( $n = 1,043$ ) (c), and genes with high variation in expression only ( $n = 4106$ ) (d). The highest ranked significant terms are shown. X-axis indicates statistical significance, with circle sizes indicating fold enrichment representing the percentage of genes within the group. All protein coding and long noncoding RNA genes were used as input. **(e, f)** Correlation between  $rGS$  and log-scaled ATAC-seq coverage in B6 (e) and CAST (f) alleles. SCC, Spearman's Correlation Coefficient. Each dot represents a unique 50kb region. **(g)** Heatmap summarizing the observed differences in gene radiality, gene expression and promoter accessibility between B6 and CAST alleles. All genes displayed in (a) are included and sorted based on classification. Here, expression  $\log_2FC$ , promoter accessibility  $\log_2FC$ , and  $\Delta rGS$  were rescaled to fall in a similar range, herein described as allelic variation intensity. **(h, i)** Correlation between differences in promoter accessibility and gene expression between B6 and CAST alleles. Each dot represents an autosomal gene with  $\Delta rGS$  above 0.2 (h) or below 0.2 (i); genes colored based on GPSeq variation. For each gene, the x-axis indicates  $\log_2FC$  between TPM values, while the y-axis indicates  $\log_2FC$  between ATAC-seq coverage observed around transcriptional start sites ( $\pm 3$  kb). TPM, transcripts per million. SCC, Spearman's Correlation Coefficient. **(j)** Distribution of accessibility differences (absolute  $\log_2FC$  between ATAC-seq coverage) depending on autosome allelic radiality. Different regions were classified as low (L) ( $rGS < 0.33$ ), medium (M) ( $rGS$  between 0.33 and 0.66) and high (H) ( $rGS > 0.66$ ) in B6 and CAST alleles,

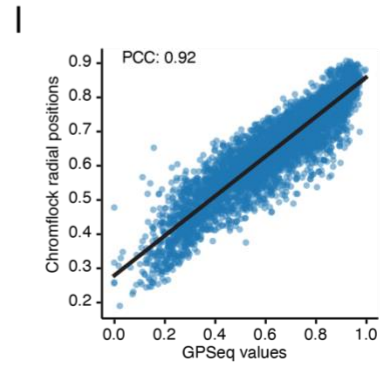
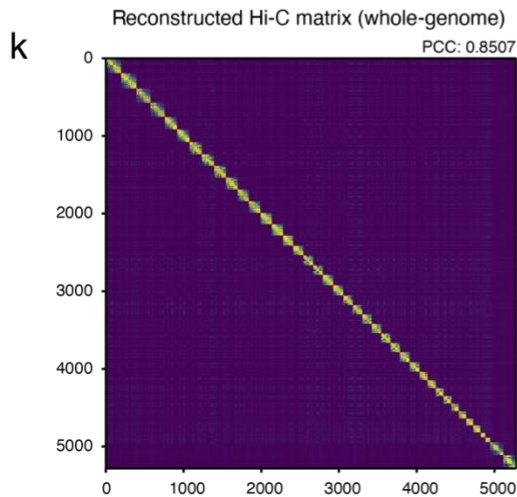
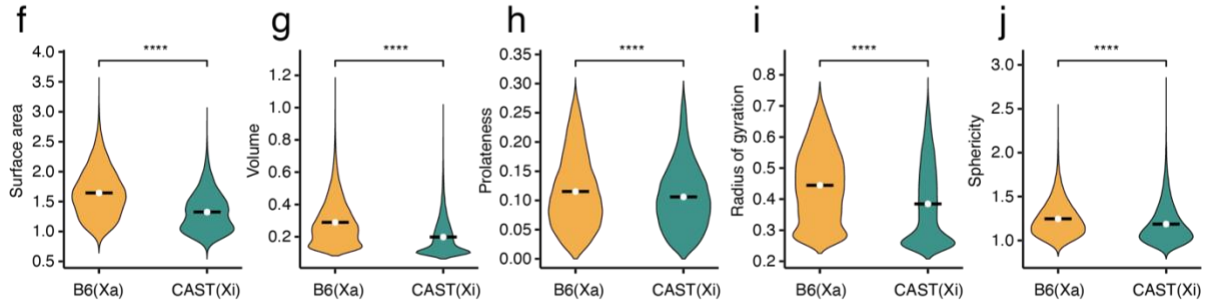
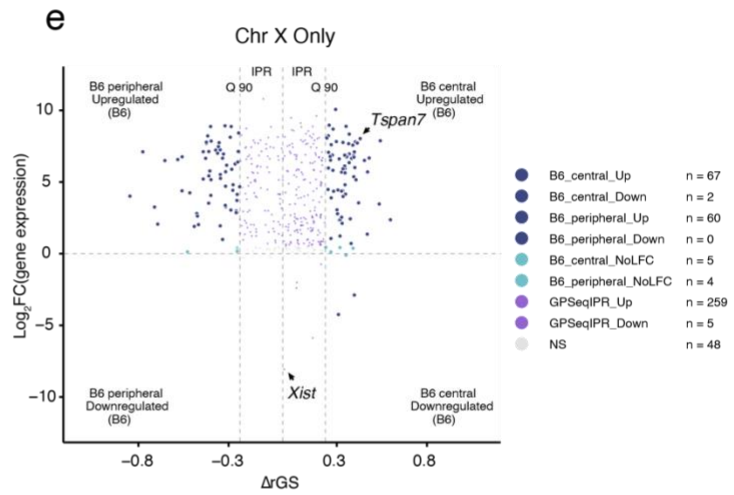
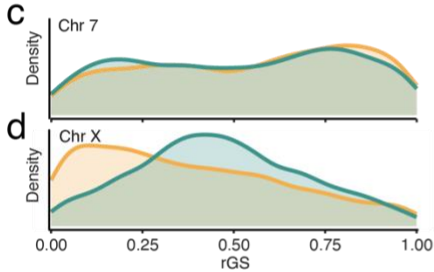
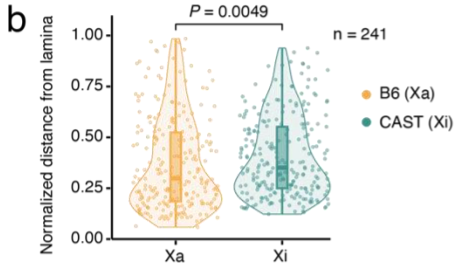
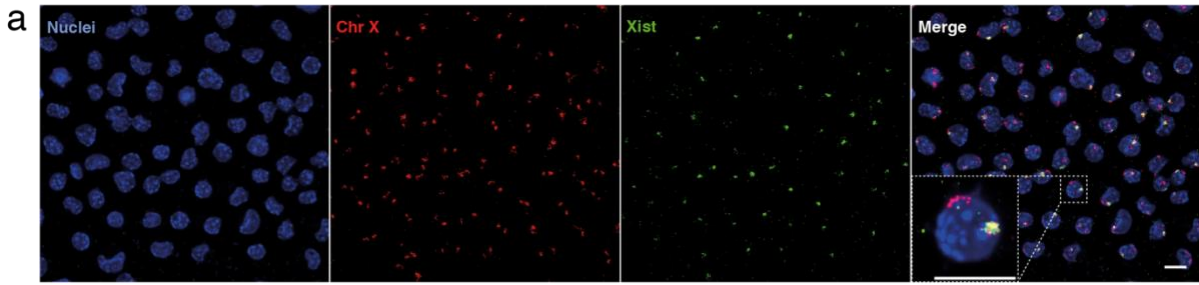
respectively. A link to the Source Data and code to regenerate the plots in this figure is provided in the Data Availability and Code Availability statements.

## Supplementary Figure 6



**Supplementary Figure 6. Sequencing coverage comparison between the Xi and Xa.** (a, b) GPSeq allele-phased coverage profiles of early (a) and late (b) DpnII digestion timepoints in Chr X. (c) ATAC-seq allele-phased coverage profile of Tn5 digestion in Chr X. (d) Hi-C allele-phased coverage profile in Chr X (intra-chromosomal interactions only). All tracks show the log-scaled number of reads per window (50 kb resolution). The B6 allele (maternal, Xa) is colored in yellow, while the CAST allele (paternal allele, Xi) is colored in green. A link to the Source Data and code to regenerate the plots in this figure is provided in the Data Availability and Code Availability statements.

# Supplementary Figure 7



**Supplementary Figure 7. Allele-specific comparisons of the X chromosomes after X chromosome inactivation.** (a) Representative microscopic images of DNA-RNA FISH. Two alleles of chromosome X are labelled by DNA FISH probes tiling the whole chromosome (red) while *Xist* RNA is marked using an RNA FISH probe (green). Nuclei are counterstained by Hoescht33342 (blue). Scale bar: 10  $\mu\text{m}$ . (b) Quantification of the normalized distance of the two alleles of chromosome X from the nuclear periphery. Each dot represents a nuclear. n, number of nuclei analyzed. P, Mann–Whitney U test, two-sided. (c, d) Distribution of ranked GPSeq score (rGS) of the two alleles of Chr 7 and Chr X at 50 kb resolution respectively. (e) Correlation scatterplot showing the relationship between differences in radial positioning and gene expression between Xa and Xi. Y-axis, gene expression  $\log_2\text{FC}$  between B6 and CAST TPM values. The x-axis shows radial positioning variation as the difference between B6 and CAST radiality ( $\Delta\text{rGS}$ ). Each dot represents one gene. Two vertical dashed lines indicate genes with the largest allelic radiality variation (above the 90<sup>th</sup> percentile, q90). IPR, inter-percentile range  $P_{90} - P_{10}$ , of the  $\Delta\text{rGS}$ . Genes are colored according to these thresholds to identify groups showing changes in both expression and radiality (dark blue), expression only (purple), radiality only (light blue), or neither/significant stability (grey). Positive and negative values refer Xa (B6). (f-j) Comparison of 3D shape features between the B6 (Xa) and CAST (Xi) alleles, for respectively surface area, volume, prolateness, radius of gyration, and sphericity, calculated for each allele of the Chr X beads in every reconstructed structure (n = 50,000). Violin plots show the distribution across structures, white points indicate the mean. Statistical significance was assessed using a two-sided Mann–Whitney U test. (k) Reconstructed Hi-C matrix at 1Mb generated from contacts measured in *Chromflock* single-cell reconstructions (n = 50,000). The reconstructed contact matrix was compared with the reference Hi-C matrix using Pearson’s correlation. (l) Pearson’s correlation between GPSeq values and radial positions of *Chromflock* beads at 1Mb. GPSeq scores were compared with the mean radial positions of *Chromflock* beads calculated across all structures. Each point corresponds to one bead. Blue line, linear regression fit. A link to the Source Data and code to regenerate the plots in this figure is provided in the Data Availability and Code Availability statements.

## **2. Supplementary Tables**

Because of their large size, all tables are provided as separate Excel files.

**Supplementary Table 1.** Summary of sequencing datasets analyzed in this study.

**Supplementary Table 2.** GPSeq scores and RNA-seq counts in mESC and mNPC.

**Supplementary Table 3.** Results of all the GO analyses described in this study.

**Supplementary Table 4.** DNA and RNA FISH probes and corresponding oligos used in this study.

**Supplementary Table 5.** Allele-resolved GPSeq scores and RNA-seq counts for X-linked genes in mNPC clone 5.

**Supplementary Table 6.** GPSeq adapters and corresponding oligos used in this study.